

Comparative Study on Bending Strength of Metallic Bone Staple

Nur Hidayatul Nadhirah Elmi Azham Shah¹, Muhammad Afiq Hanizar¹, Muhammad Hussain Ismail^{1*}

¹Industrial Metallurgy Research Group (IMReG), Faculty of Mechanical Engineering, Universiti Teknologi MARA (UiTM), 40450 Shah Alam, Selangor, MALAYSIA

*Corresponding author E-mail: hussain.305@salam.uitm.edu.my

Abstract

This study compares bending behavior of metallic bone staples made with different metallic alloys; SS316L, CpTi and Ti40Nb. The staples were prepared by EDM wire cut in accordance with ASTM F564-10, standard specification and test methods for metallic bone staples. The materials of SS316L and CpTi were initially obtained from commercial rod, while the Ti40Nb alloy was manufactured by powder metallurgy (PM) process. Through this comparative study, development and feasibility of Ti40Nb, a β -rich TiNb alloy performance as a biomedical device specifically bone staple is studied. In the four point bending test, the data obtained for the metallic staple bending strength were 11.16 ± 1.57 N/mm, 12.22 ± 1.77 N/mm and 6.76 ± 0.46 N/mm for SS316, CpTi and Ti40Nb, respectively. Only Ti40Nb experience failure whereas SS316 and CpTi bone staples suffers permanent deformation without failure.

Keywords: Bending strength; bone staple; stainless steel; titanium alloy.

1. Introduction

Improved surgical and clinical outcomes can be achieved with the help of internal fixation devices such as staples, plates, screws, pins and cerclage wires which provides rigidity and stability to the affected area. Staple fixations were among the common fixation system employed in foot and ankle surgery [1], [2]. Conceptually, a bone staple is a single fixation device consisted of 2 or more point of entries into a bone that were joined together [3].

In the light of the latest trends in staple fixation system is the usage of dynamic compression staples [4]. Commercially, these staples are known for the ability to provide compression in the bone fixation sites and can be activated via heat. These compression staples are made of shape memory alloys such as NiTi. Compression staples provide an option where there is less bulky hardware and complications in comparison to more frequently used method of fixations such as plates and screws [5]. Figure 1 is an X-ray of foot before (top) and after (bottom) a hallux interphalangeal joint fusion with a staple shown in a Podiatry Today article [5]. A unique advantage of a less bulky hardware is better visualization of fusion site on postoperative X-ray, which allows better assessment of bone healing process [5].

From the biocompatibility point of view, adverse biological reaction which occurs with the usage of commercialized implants becomes the main concern when dealing with the research and development of new implant materials. Implant materials such as Ti6Al4V and NiTi [6], [7] are both widely used and recognized. However, there is a risk of inflicting negative impact to the patient receiving Ti6Al4V and NiTi implants caused by the presence of Al and Ni due to the elemental toxicity risk [8]–[10]. This toxicity issue helps to propel the research made on Al and Ni free Ti alloys for implant application. Niobium (Nb) is one of many alternatives for Al and Ni free Ti alloy [11]–[13]. Table 1 is a summarization of common elements usually used in the production of implants

and medical instruments and their level of harmfulness to the human body, adapted from Kuroda et al [9].



Fig. 1: X-ray of foot before (top) and after (bottom) a hallux interphalangeal joint fusion with a staple [5].

Table 1: Summarization of elemental biocompatibility

- Biocompatibility →		
Toxic	Capsule	Vital
V	Co-Cr alloy	Zr
Ni	316L	Ti

Cu	304L	Nb
Co	Au	Ta
	Al Mo	Pt
	Fe	

Mechanical compatibility is another factor that is equally important as biocompatibility in selecting and designing an implant material. Stiffness mismatch between bone and implant material will cause stress shielding effect which eventually leads to implant failure [13], [14]. Stress shielding causes a decrease in bone density surrounding the implant which eventually loosens the implant, leading to implant failure. In avoiding stress shielding, the stiffness value of the implant material needs to be comparable to the human bone. For instance, the Young's modulus of the bone (human cortical bone is 15-30 GPa and that of human spongy bone is around 0.2-2 GPa [9]) is significantly lower in comparison to the Young's modulus of the commercially available implant (112 GPa for Ti-6Al-4V and ≈ 100 GPa for commercially pure Ti) [15]. Table 2 is the mechanical properties of metallic implant materials and cortical bone [16]

Table 2: Mechanical properties of metallic implant material and cortical bone [16]

Materials	Young's modulus, (GPa)	UTS (MPa)
CoCrMo alloys	240	900-1540
316l stainless steel	200	540-1000
Ti alloys	105-125	900
Mg alloys	40-45	100-250
NiTi alloys	30-50	1355
Cortical bone	10-30	130-150

With regards to the processing technique, the biggest hurdle when working with Ti-based alloy is the high sensitivity of Ti towards impurity uptake, particularly carbon and oxygen. Conventional casting followed by machining process is the traditional method in fabricating products of Ti-based alloy. Casting technique requires several remelting to attain homogeneous structure. Currently, there are quite number of research synthesizing new alloy via powder metallurgy owing to the advantage of the process in producing near-net-shape component with flexible design, which is significant for small and intricate shape of medical implants. Utilizing elemental or pre-alloyed metallic powders, in a simple powder metallurgy route, the powders may be mixed and then compacted followed by a sintering process. In producing Ti based products by PM process, the compacted parts, so called green parts need to be sintered in a high vacuum atmosphere in order to minimize the uptake of impurities. Besides, an alternative to vacuum sintering is currently being investigated by performing sintering of Ti alloy in an argon flow furnace incorporated with reducing agent materials. This reducing agent acts as barrier to cover the surface of the parts from being contaminated during sintering. Impurities, predominantly carbon and oxygen, might be deposited on the powder surface, along with the formation of intermetallic phases originated from different diffusivity levels of elements in Ti alloys which inhibits further densification during sintering.

For the purpose of this study, water atomized Ti and Nb elemental powders were utilized to develop binary β -rich Titanium 40wt% Niobium (Ti40Nb) alloy. This study attempts to investigate the behavior of TiNb alloy along with commercially pure Ti (CpTi) and stainless steel 316 (SS316L). The sintering process in this study utilizes argon gas atmosphere for sintering process using a simple tube furnace.

For preparation of samples, the metallic bone staple of SS316, CpTi and Ti40Nb were made and tested via four point bend test and the main objective is the development and feasibility of β -rich TiNb alloy (produced via powder metallurgy and sintered in argon atmosphere) performance as a biomedical device specifically bone staple.

2. Experimental Procedure

Three metallic materials were utilized in this experiment. The raw materials of SS316L and CpTi were obtained from the commercially rods, while Ti40Nb alloy was prepared by the powder metallurgy (PM) process.

In the processing of TiNb alloy, the Ti and Nb elemental powders with average particle size of 68 μm and 132 μm , respectively, were ball milled into Ti40Nb (wt%) using 2:1 ball to powder weight ratio with a total of 2 hours milling time. The powder mix was compacted into a cylindrical mould using a 10 tonne press machine at room temperature, followed by cold-isostatic press (CIP) to uniform the packing density. The green parts were then sintered in a tube furnace with argon gas atmosphere incorporated with CaH_2 as a reducing agent. The samples were placed in alumina crucible with yttria plate. The sintering process consisted of heating to 800°C from room temperature with heating rate of 2°C/min and holding for 1 hour for CaH_2 decomposition before hiking up the temperature to 1200°C with heating rate of 5°C/min and holding for 4 hours. The samples were furnace cooled to room temperature.

The SS316 rod, CpTi rod and sintered Ti40Nb were cut into staples and underwent Scanning Electron Microscopy (SEM) and Energy-dispersive X-ray spectroscopy (EDX) analysis, four point bend test in accordance with ASTM F564-10[17] and hardness test.

3. Results and Discussion

3.1. Physical Properties of the Sample

Bone staples which were made for the current study utilized a simple staple design with toothed legs. This design was made with reference to staples produced by commercial bone implant produced by BioMedical Enterprise[18].

Figure 2 shows the measurements of the metallic bone staple whereas Figure 3 shows the actual metallic bone staple produced after EDM wire cut process.

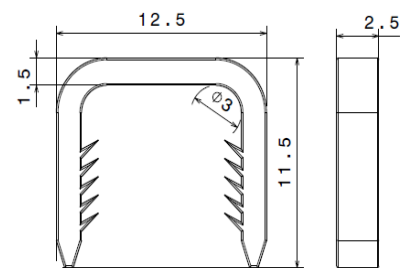


Fig. 2: Measurements of metallic bone staple implant in mm

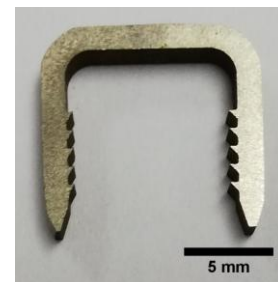


Fig. 3: Metallic bone staple produced after EDM wirecut process

3.2. SEM and EDX

SEM analysis was performed for all metallic bone staples. Figure 4 to 6 show the microstructures of the metallic materials investigated in the present study and their respective EDX spectra. The

microstructure of SS316L in Figure 4 clearly shows common austenitic stainless steel microstructure. As shown in the EDX spectra SS316L is a grade of stainless steel with molybdenum (Mo) content which results in a good corrosion resistance. CpTi microstructure as in Figure 5 shows an overall hexagonal closed packed (hcp) α -Ti phase. Being a commercially pure grade Ti, CpTi contains no alloying elements but have some other trace elements as shown in the EDX spectra. The microstructure Ti40Nb alloy as shown in Figure 6 consists of primarily β -Ti matrix with fragmented and acicular α -Ti phase. As shown in the EDX spectra, Ti40Nb consists primarily of Ti and Nb elements.

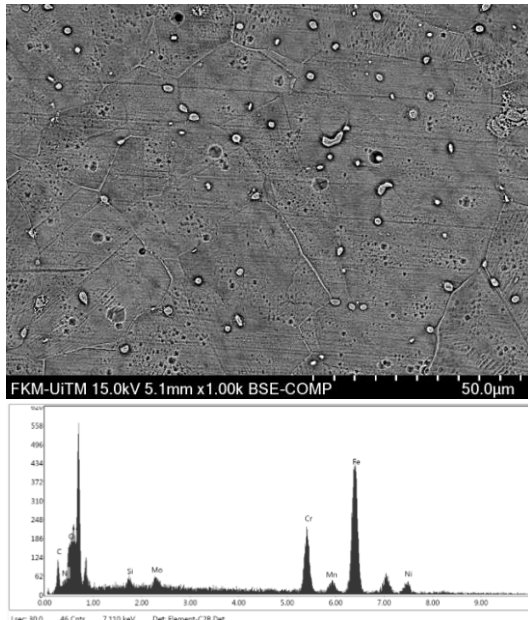


Fig. 4: Microstructure of SS316L and EDX spectra

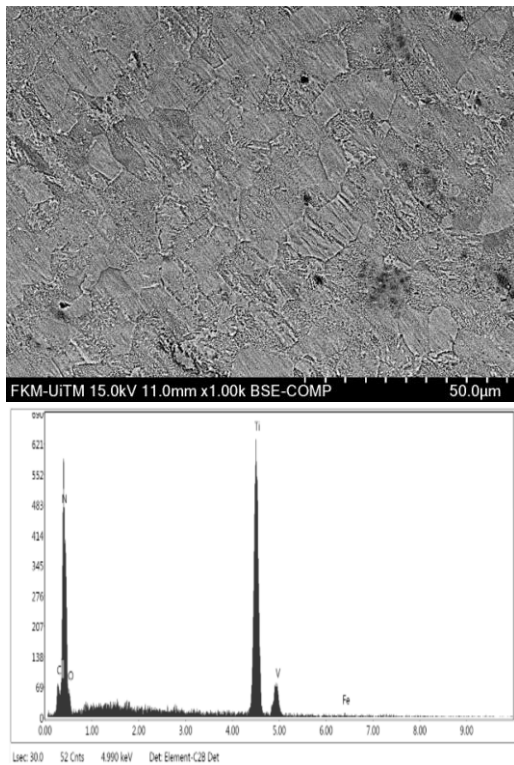


Fig. 5: Microstructure of CpTi and EDX spectra

Overall, since the micrographs were taken at similar magnification, it is obvious that CpTi had the smallest grain size compared to the SS316L and Ti40Nb. In terms of structure, both SS316 and CpTi are solids and does not contain porosity, however, on the other

hand Ti40Nb have several clustered porosities and contains open and closed pores, which is seen as several dark spots in the microstructure.

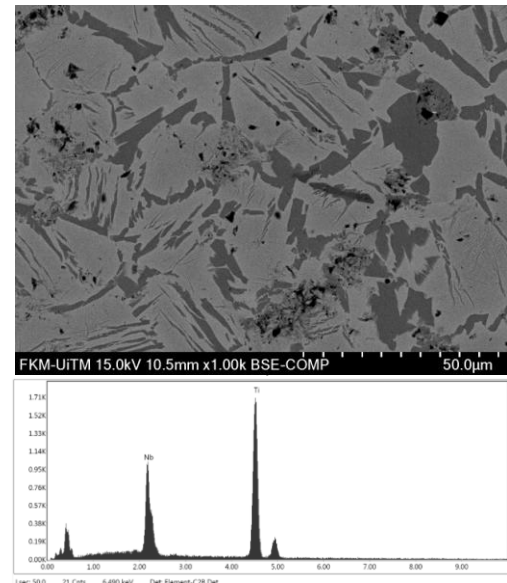


Fig. 6: Microstructure of Ti40Nb and EDX spectra

3.3. Four Point Bend Test

ASTM F564-10, standard specification and test methods for metallic bone staples was utilized to test the elastic static bending of the metallic bone staples. Four point bend test was performed on several staples to obtain an average bending strength. In performing the test, the bone staple was fixated into an extension made of rigid stainless steel jig. Grub screws were used to hold the metallic bone staple in place for the testing process. This process is in accordance to ASTM F564-10. Figure 7 shows the assembly for the metallic bone staple and loading during four point bend test.

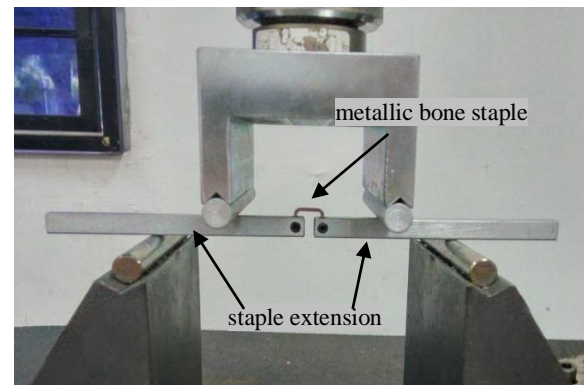


Fig. 7: Assembly for the metallic bone staple and loading during four point bend test

Metallic bone staples made of SS316L, CpTi and Ti40Nb all shows a variation of condition after the four point bend test. SS316L and CpTi staples exhibited permanently plastic deformation with no failure at the end of the test with CpTi showing less bending compared to SS316L samples. However Ti40Nb staple experience failure at the end of the test. This is due to the nature of the metallic elements as CpTi is made up of α -Ti with very high strength and stiffness value, followed by SS316L and lastly Ti40Nb which is made up of β -Ti with very low stiffness value [19]. The porosities in Ti40Nb staple also may influence the staple bending strength. Figure 8 shows the condition of the metallic staples after performing four point bend test.

The staple stiffness was calculated by measuring the initial slope of load-displacement curve and measured by the unit N/mm[17].

Load-displacement curve of metallic bone staples made from SS316, CpTi and Ti40Nb were made as in Figure 9. Figure 9 shows an example of load displacement curve for each metallic material. In performing the four point bend test, three staples were made for each metallic element to obtain an average value of staple stiffness.

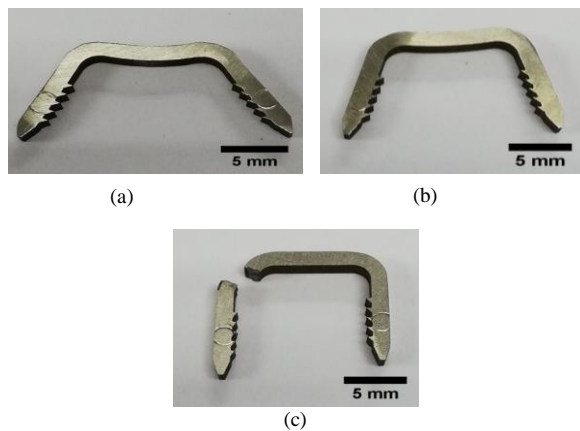


Fig.8: Metallic staples after four point bend test (a) SS316 (b) CpTi and (c) Ti40Nb

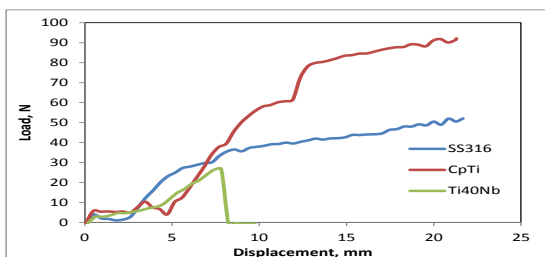


Fig. 9: Load displacement curve of SS316, CpTi and Ti40Nb bone staple

From the Figure 8, it is obvious that SS316L and CpTi staples are able to withstand high amount of load compared to Ti40Nb staple which experience failure at the displacement of 7.82 mm and load of 26.71 N. They both were able to withstand up to 20 mm of displacement and only sustain permanent deformation without bending failure.

In terms of the staple bending strength, a comparative bar chart is used as in Figure 10 to show the difference between the metallic bone staples. As shown in Figure 10, the staple bending strength of the current study is highest in CpTi followed by SS316L and Ti40Nb with the values of 12.22 ± 1.77 N/mm, 11.16 ± 1.57 N/mm and 6.76 ± 0.46 N/mm respectively. Two examples of commercially used staples produced by BioMedical Enterprises and Wright Medical Group were also placed in the graph to provide a more pronounced outlook on the common values of metallic staple bending strength.

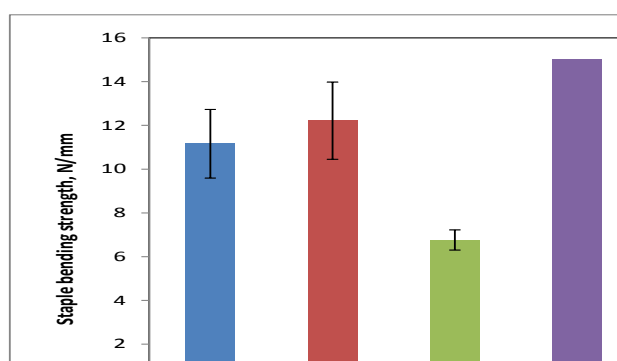


Fig. 10: Bending strength of the current study SS316L, CpTi and Ti40Nb bone staples and commercial bone staples [18], [20]

3.4. Vickers Hardness

In obtaining more information on the mechanical properties of the bone staples Vickers hardness test was also performed which is presented in Figure 11.

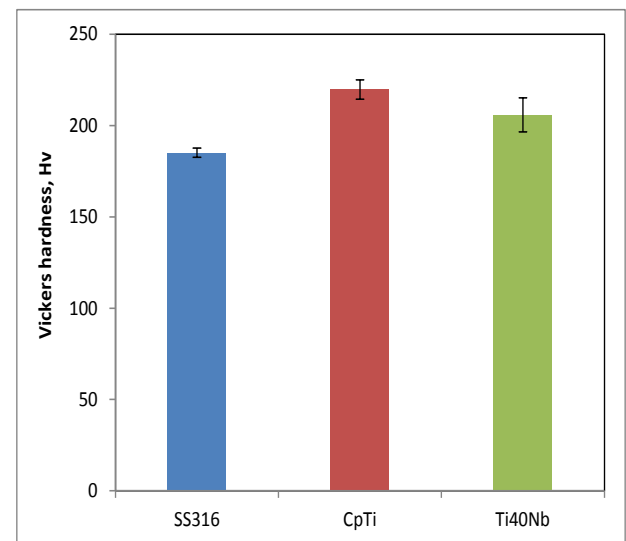


Fig. 11: Vickers hardness value of SS316, CpTi and Ti40Nb

Based on the Vickers hardness values, there is only small difference in hardness between the samples as the highest value was taken from CpTi is 219.66 ± 2.53 HV, followed by Ti40Nb 205.74 ± 9.3 HV and the lowest from SS316L 185.08 ± 2.53 Hv. Overall CpTi is the hardest and SS316L is the softest amongs the metallic bone staple, however these hardness values might not have much influence over the bending strength of the metallic bone staple.

4. Conclusions

The result of SEM and EDX test on the SS316L, CpTi and Ti40Nb metallic bone staple verifies the material of the bone staples and also its elemental constituents. In the four point bending test, the data obtained for the metallic bone staple bending strength are 11.16 ± 1.57 N/mm, 12.22 ± 1.77 N/mm and 6.76 ± 0.46 N/mm for SS316L, CpTi and Ti40Nb respectively. Only Ti40Nb experience failure whereas SS316L and CpTi bone staples suffers permanent deformation but no failure. The value of staple bending strength of Ti40Nb is significantly low compared to the other two materials in the current study and also existing commercially used bone staples. In terms of hardness value, Ti40Nb have comparable hardness to CpTi, however, hardness may play an insignificant role in the staple bending strength. This study only touches a small part of ASTM F564-10 standard specification and test methods for metallic bone staples. Overall, there is a large area of improvement that could be performed and more research is required to turn Ti40Nb into a metallic bone staple fit for commercialization. Future improvements such as the implementation of heat treatment or coating system would definitely enhance the performance of Ti40Nb metallic bone staple.

Acknowledgement

This work is funded by the Fundamental Research Grant Scheme (FRGS) of Kementerian Pendidikan Malaysia (KPM) under the project titled Stabilizer Niobium Nanoparticle in Beta Phase Pulverized Titanium Metal (Project code: FRGS/1/2014/TK04/JPP/03/1).

References

- [1] Q. J. Hoon, M. H. Pelletier, C. Christou, K. A. Johnson, and W. R. Walsh, "Biomechanical evaluation of shape-memory alloy staples for internal fixation—an in vitro study," *J. Exp. Orthop.*, vol. 3, no. 1, (2016), p. 19.
- [2] A. F. Saleeb, B. Dhakal, and J. S. Owusu-Danquah, "Assessing the performance characteristics and clinical forces in simulated shape memory bone staple surgical procedure: The significance of SMA material model," *Comput. Biol. Med.*, vol. 62, (2015), pp. 185–195.
- [3] T. F. Smith, *The Podiatry Institute Update Chapters : Chapter 41 - Tried and True Superhero of Bone Fixation.* (2010).
- [4] Z. Lekston, D. Stroz, and M. J. Drusik-Pawlowska, "Preparation and characterization of nitinol bone staples for cranio-maxillofacial surgery," *J. Mater. Eng. Perform.*, vol. 21, no. 12, (2012), pp. 2650–2656.
- [5] T. A. Harris, "Emerging Concepts With Dynamic Compression Staples In Foot Surgery," *Pod. Today*, vol. 30, no. 3, (2017), pp. 1–5.
- [6] M. H. Ismail, R. Goodall, H. a. Davies, and I. Todd, "Porous NiTi alloy by metal injection moulding/sintering of elemental powders: Effect of sintering temperature," *Mater. Lett.*, vol. 70, (2012), pp. 142–145.
- [7] M. I. Jamaludin, N. A. A. Kasim, N. H. M. Nor, and M. H. Ismail, "Development of porous Ti-6Al-4V Mix with palm stearin binder by metal injection molding technique," *Am. J. Appl. Sci.*, vol. 12, no. 10, (2015), pp. 742–751.
- [8] N. H. N. Elmi Azham Shah, M. Yahaya, M. Sulaiman, and M. H. Ismail, "a Metallurgical Overview of Ti – Based Alloy in Biomedical Applications," *J. Teknol.*, vol. 76, no. 7, (2015).
- [9] D. Kuroda, M. Niinomi, M. Morinaga, Y. Kato, and T. Yashiro, "Design and mechanical properties of new β type titanium alloys for implant materials," *Mater. Sci. Eng. A*, vol. 243, no. 1–2, (1998), pp. 244–249.
- [10] P. Thomas *et al.*, "Increased metal allergy in patients with failed metal-on-metal hip arthroplasty and peri-implant T-lymphocytic inflammation," *Allergy Eur. J. Allergy Clin. Immunol.*, vol. 64, no. 8, (2009), pp. 1157–1165.
- [11] B. Sharma, S. K. Vajpai, and K. Ameyama, "Microstructure and properties of beta Ti-Nb alloy prepared by powder metallurgy route using titanium hydride powder," *J. Alloys Compd.*, vol. 656, (2015), pp. 978–986.
- [12] M. Bönisch *et al.*, "Thermal stability and latent heat of Nb-rich martensitic Ti-Nb alloys," *J. Alloys Compd.*, vol. 697, (2017), pp. 300–309.
- [13] D. Zhao, K. Chang, T. Ebel, H. Nie, R. Willumeit, and F. Pyczak, "Sintering behavior and mechanical properties of a metal injection molded Ti-Nb binary alloy as biomaterial," *J. Alloys Compd.*, vol. 640, (2015), pp. 393–400.
- [14] É. S. N. Lopes, C. A. F. Salvador, D. R. Andrade, A. Cremasco, K. N. Campo, and R. Caram, "Microstructure, Mechanical Properties, and Electrochemical Behavior of Ti-Nb-Fe Alloys Applied as Biomaterials," *Metall. Mater. Trans. A*, vol. 47, no. 6, (2016), pp. 3213–3226.
- [15] M. Geetha, a. K. Singh, R. Asokamani, and a. K. Gogia, "Ti based biomaterials, the ultimate choice for orthopaedic implants - A review," *Prog. Mater. Sci.*, vol. 54, no. 3, (2009), pp. 397–425.
- [16] M. Long and H. J. Rack, "Titanium alloys in total joint replacement—a materials science perspective," *Biomaterials*, vol. 19, no. 18, (1998), pp. 1621–1639.
- [17] ASTM International, "Standard Specification and Test Methods for Metallic Bone Staples," *Astm F564-10(2015)*, vol. 03, no. Reapproved, (2015), pp. 1–18.
- [18] BioMedical Enterprises, "Speed Titan Datasheet," San Antonio, TX, (2016).
- [19] M. Yahaya, S. Sahidin@Salehudin, M. Sulaiman, N. H. N. E. Azham Shah, and M. H. Ismail, "Microstructures and Mechanical Properties of Ti-Nb Alloy at Different Composition of Nb Produced via Powder Metallurgy Route," *Mater. Sci. Forum*, vol. 863, (2016), pp. 14–18.
- [20] Wright Medical Group, "Charlotte™ claw™ Compression Locking Arthrodesis," Memphis, TN, (2016).